Lifshitz Transitions in the Ferromagnetic Superconductor UCoGe

Gaël Bastien,[1,2,*] Adrien Gourgout,[1,2] Dai Aoki,[1,2,3] Alexandre Pourret,[1,2]
Ilya Sheikin,[4] Gabriel Seyfarth,[4] Jacques Flouquet,[1,2] and Georg Knebel[1,2,†]

[1] *University Grenoble Alpes, INAC-PHELIQS, F-38000 Grenoble, France*
[2] *CEA, INAC-PHELIQS, F-38000 Grenoble, France*
[3] *IMR, Tohoku University, Oarai, Ibaraki 311-1313, Japan*
[4] *LNCMI-EMFL, CNRS, UGA, F-38000 Grenoble, France*

(Dated: September 28, 2016)

We present high field magnetoresistance, Hall effect and thermopower measurements in the Ising-type ferromagnetic superconductor UCoGe. Magnetic field is applied along the easy magnetization c axis of the orthorhombic crystal. In the different experimental probes we observed five successive anomalies at $H \approx 4$, 9, 12, 16, and 21 T. Magnetic quantum oscillations were detected both in resistivity and thermoelectric power. At most of the anomalies, significant changes of the oscillation frequencies and the effective masses have been observed indicating successive Fermi surface instabilities induced by the strong magnetic polarization under magnetic field.

PACS numbers: 71.27.+a, 71.18.+y, 71.20.-b, 74.70.Tx

arXiv:1609.08466v1 [cond-mat.str-el] 27 Sep 2016

Lifshitz transitions (LTs) are continuous quantum phase transitions at zero temperature where the topology of the Fermi surface (FS) changes due to the variation of the Fermi energy and the band structure of a metal [1, 2]. They have been already studied in the sixties and can be induced by chemical doping, pressure, or strong magnetic field (H). However, only recently LTs have been proposed as the driving force to modify the ground-state properties in strongly correlated electron systems. The interplay of a LT with magnetic quantum phase transitions in heavy fermion systems has been treated in various theoretical models (see e.g. Refs. 3–8). The influence of LTs on the appearance of superconductivity is discussed in cuprates [9, 10], iron pnictides [11, 12] sulfur hydride [13] and also for the reentrance of superconductivity in URhGe [14]. Finally, LTs play an important role in topological insulators [15] or in the vortex state of ^{3}He [16].

Usually the electronic band structure is a rather robust property of the metallic state, especially when applying magnetic fields. Only when the magnetic ground state is modified, changes of the FS may be detected. In a normal metal the Zeeman splitting induced by accessible magnetic fields is weak with respect to the Fermi energy which is usually of the order of a few eV. Importantly, in heavy fermion compounds the Fermi energy scale is significantly reduced due to the hybridization of the conduction and the localized f electrons. Thus, the Zeeman splitting of the flat bands crossing the Fermi level can be so strong that one of the spin-split FS sheets is continuously suppressed and undergoes a LT. In heavy-fermion systems a LT is often associated to a change in the intersite and/or local magnetic fluctuations, see e.g. in $CeRu_2Si_2$ [17], $CeIn_3$ [18, 19], $YbRh_2Si_2$ [20–22].

In this Letter we report on FS properties of UCoGe under magnetic field, which orders ferromagnetically at $T_C = 2.7$ K. Remarkably, homogeneous coexistence of ferromagnetism and heavy-fermion superconductivity is observed below $T_{sc} = 0.6$ K [23]. UCoGe crystallizes in an orthorhombic structure (space group $Pnma$). Besides the exceptional superconducting properties [24] some normal state features of UCoGe are unique. The spontaneous magnetization in the ferromagnetic (FM) state is very small, $M_0 \approx 0.05\,\mu_B$/U with Ising moments along the c axis [25] and under magnetic field the magnetization is strongly anisotropic with $M_c > M_b > M_a$. For $H \parallel c$, M_c increases non-linearly with field and shows a broad kink at $H \approx 23$ T, but even at $H \sim 50$ T, with $M_c \approx 0.65\,\mu_B$/U at $T = 1.5$ K, it is far from saturation [26]. Another striking point is the detection of well separated anomalies in the magnetoresistance for $H \parallel c$ [27–29] far above the collapse of the FM fluctuations ($H > 1$ T) [30] while $M(H)$ rules out thermodynamic phase transitions under magnetic field at least down to 1.5 K [26].

In order to study the field dependence of the FS properties in a highly polarizable heavy fermion system with small FS pockets we performed systematic resistivity (ρ), Hall effect (ρ_{xy}) and thermopower (S) experiments in UCoGe. Two different samples (labelled S1 and S2) with residual resistivity ratios [$RRR = \rho(300\,\mathrm{K})/\rho(1\,\mathrm{K})$] of 105 and 36 have been prepared for experiments with electrical or heat current along the b and a axis respectively. Details of the experiments are given in the Supplemental Material [31].

Figure 1 shows the field dependence of ρ_{xy} at 40 mK and thermopower at 900 mK and 450 mK along the c axis for S1. At least five successive anomalies can be observed above the superconducting critical field $H_{c2} \approx 0.6$ T in both probes. $S(H)$ exhibits successive marked minima at $H_1 \approx 3.65$ T, $H_2 \approx 9.2$ T, and $H_4 \approx 16$ T. A shoulder like anomaly appears at $H_3 \approx 12$ T and a small kink at $H_5 \approx 21$ T. At 450 mK, in addition, large quantum oscillations occur in the thermopower (see below). At all these

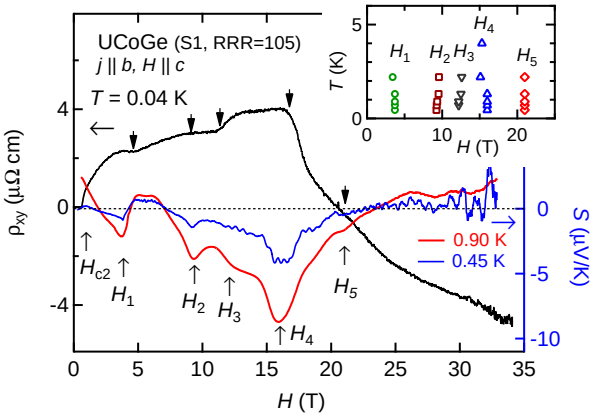

FIG. 1. (Color online) Hall effect ρ_{xy} at 40 mK (left scale) and thermopower S at 900 mK and 450 mK (right scale) of UCoGe as a function of magnetic field. A series of transitions can be observed as a function of field. The inset shows the temperature dependence of the anomalies in the thermopower.

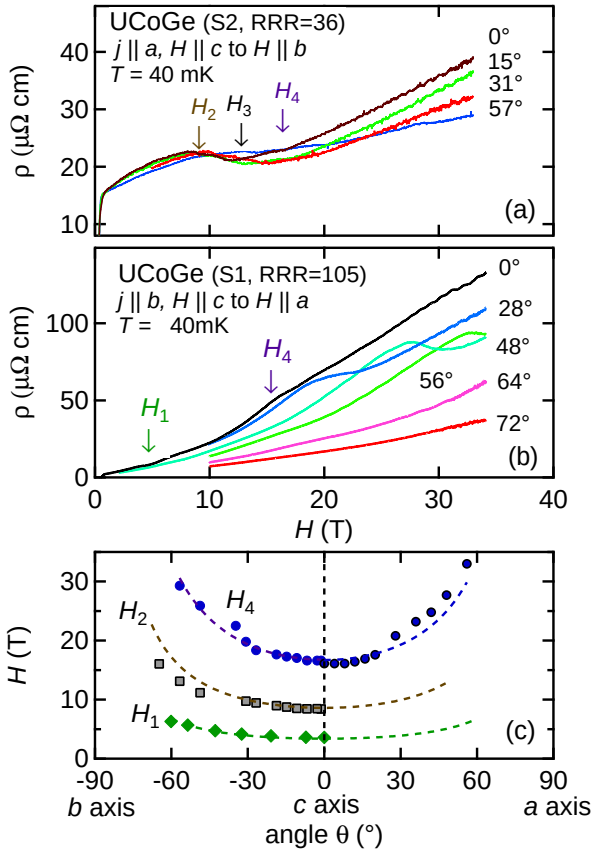

FIG. 2. (Color online) Transverse magnetoresistance at $T = 40$ mK in UCoGe with (a) current along a axis on sample S2 for different angles in the bc plane and (b) current along b on S1 in the ac plane. The arrows indicate the position of the anomalies for 0° along the c axis. (c) Angular dependence of the anomalies at H_1, H_2, and H_4. Dashed lines are fits with $H \propto 1/\cos\theta$.

characteristic fields $\rho_{xy}(H)$ shows rather sharp anomalies with step-like increases or kinks. At $H_4 = 16$ T the most pronounced anomaly is observed and $\rho_{xy}(H)$ decreases abruptly, whereas $S(H)$ has a marked minimum and increases for higher fields. In the whole field range ρ_{xy} and S have opposite sign, which changes around 22 T suggesting a change of the dominant carrier type [34]. The temperature dependence of the anomalies observed in $S(H)$ is shown in the inset of Fig. 1. The transitions get less pronounced with increasing temperature and disappear above $T \approx 3$ K while their field position does not change. The clear signatures of these transitions in transport properties $\rho_{xy}(H)$ and $S(H)$ and the absence of any marked phase transition in thermodynamic properties [26, 35] suggest that they are related to topological FS changes.

Figure 2 shows the transverse magnetoresistance $\rho(H)$ of UCoGe up to 34 T (a) in the bc plane with current along the a axis (S2) and (b) in the ac plane with current along b (S1). The $\rho(H)$ shows in both configurations several anomalies and at high field quantum oscillations can be resolved. For $j \parallel a$ [see Fig. 2(a)] the resistivity shows a broad maximum around $H_2 \approx 9$ T and a minimum at $H_3 \approx 12$ T. A tiny kink can also be observed at $H_4 \approx 16$ T. The magnetoresistance of S1 with current direction $j \parallel b$ is represented in Fig. 2(b) and $\rho(H)$ increases by more than one order of magnitude between 0 and 34 T. Here, $\rho(H)$ is dominated by the orbital effect in the high quality sample S1. Clear anomalies at H_1 and H_4 were detected, while no clear indication of H_2 and H_3 is seen. Previously $\rho(H)$ has been reported in Ref. 29 on a sample with $RRR = 30$ and current along the b axis. The reported field dependence along the c axis is very different from that found in the very high quality sample S1 while it is similar to that found on S2 with the current along the a axis and similar RRR suggesting that $\rho(H)$ is strongly sample dependent.

In order to investigate the anisotropy of the detected anomalies we turned the samples in the bc and in the ac plane, while keeping the transverse configuration in both cases. The rotation of S2 in the bc plane shows a shift of the anomalies H_2 and H_4 to higher fields which can be followed up to a field angle of $\theta \approx 60°$. In the ac plane $\rho(H)$ is strongly reduced when the field is rotated from the easy c axis to the hard a axis and H_3 increases with angle from the c axis. While the anomaly at H_4 smears out by rotating the field from the c axis toward the b axis, it gets more pronounced by rotating field towards the a axis and at 48° a broad maximum in $\rho(H)$ appears at H_4. Figure 2(c) shows the angular dependence of the anomalies in bc and ac planes. The angular dependence of H_1 in the bc plane was determined by thermopower. The anomalies follow quite well $1/\cos\theta$ dependence for both rotation axes and thus depend mainly on the c axis

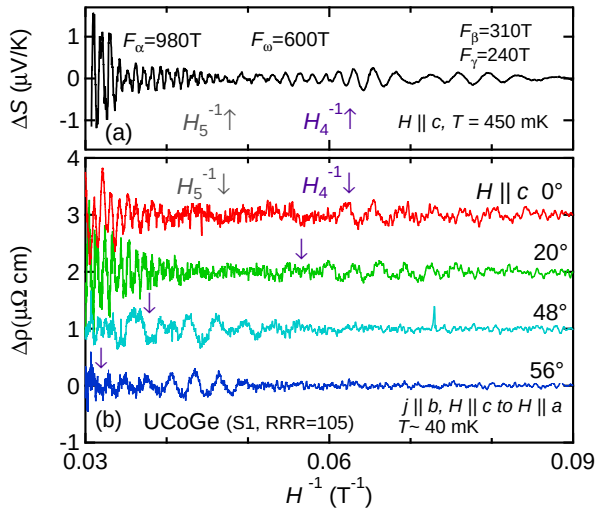

FIG. 3. (Color online) Quantum oscillations in UCoGe extracted from (a) thermopower and (b) resistivity as a function of inverse magnetic field. The arrows show the positions of H_4 and H_5 anomalies detected in transport measurements. The lower panel (b) shows also quantum oscillations in the ac plane measured by resistivity.

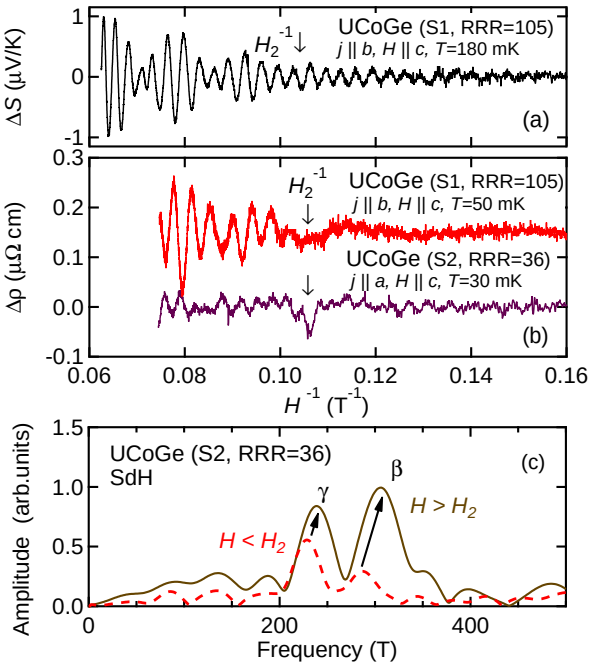

FIG. 4. (Color online) Quantum oscillations below 16T as a function of inverse magnetic field for (a) thermopower and (b) resistivity measured more precisely in a superconducting magnet. (c) FFT spectrum of quantum oscillations in the resistivity of sample S2 for field along c axis below and above $H_2 \approx 9$ T.

component of the magnetic field. For H_2 good agreement with previous reports is observed [28, 29, 36]. For both samples, Shubnikov-de Haas (SdH) oscillations could be observed in the magnetoresistance.

Figure 3 shows the oscillatory part after subtraction of a non-oscillatory background (see Supplemental Material) of (a) the thermopower and (b) of the magnetoresistance of S1 for different angles in the ac plane. For $H < 16$ T slow oscillations were observed with two very close frequencies at 240 T and 310 T. These low frequencies vanish at H_4 and faster oscillations with a frequency of $F_\omega = 600$ T appear above $H_4 = 16$ T but disappear again at $H_5 = 21$ T in the thermopower. No SdH oscillations were observed between H_4 and H_5. Above H_5 a higher frequency F_α=970 T called α branch occurs in both probes and it corresponds to that previously reported in Ref. 36.

The frequency of the quantum oscillations and the corresponding effective masses in the different field intervals are reported in Table 1 of the Supplemental Material. Figure 3 (b) shows SdH oscillations at different angles in the ac plane. While H_3 increases to higher field when approaching the a axis [see Fig. 2(c)], the oscillations at F_γ and F_β are suppressed at H_4 at each angle. At 56° a continuous increase of F_γ with field can be observed, when field gets close to the anomaly $H_4(56°) = 33$ T. This suggests that the FS pocket of the γ branch shrinks continuously, when the field gets close to the FS reconstruction field $H_4(56°) = 33$ T. Such a continuous change of a quantum oscillation frequency could not be observed clearly for the other field directions.

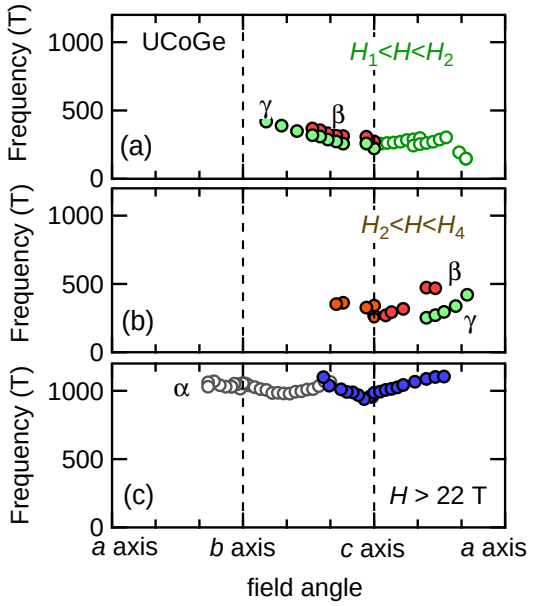

FIG. 5. (Color online) Angular dependence of quantum oscillation frequencies in UCoGe for the different field intervals delimited by the anomalies observed in transport measurements. Open circles in (a) and (c) have been taken from Ref. 36.

Quantum oscillations below H_4=16 T are represented in Fig. 4. Above H_2, a modulation of the amplitude of the oscillations in thermopower can be observed due to beating of two close quantum oscillation frequencies F_β and F_γ. While S1 shows large oscillations above H_2, the SdH oscillations below 10 T are more visible on S2. The fast Fourier transformation (FFT) spectra of the oscillations for S2 are represented in Fig. 4(c), both for field below and above H_2. Two frequencies can be observed below H_2 at 230 T and 280 T. For $H > H_2$ these two frequencies are shifted to 240 T and 310 T. A previous dHvA study suggested a splitting of one frequency from below to above H_2 [37]. On the contrary, our measurements show that both quantum oscillation frequencies survive below H_2 within the resolution of the FFT. Thus a small abrupt change in the size of the FS is directly observed by quantum oscillations at the anomaly $H_2 = 9$ T.

The angular dependence of the oscillation frequencies for the different field intervals are represented in Fig. 5. Data in the vicinity of the b axis are taken from Ref. 37 and connect perfectly to those presented here. At low field $H < H_2$, two small FS pockets elongated along the c axis (ellipsoidal or cylindrical) exist. These pockets change in size at H_2, but disappear abruptly above H_4. The angular dependence of the frequency at $F_\omega = 600$ T has not been measured. The pocket α with the heavy effective mass ranging from 17 to 23 m_0 seems to be nearly spherical with a frequency around $F_\alpha \approx 1000$ T [Fig. 5(c)] and is experimentally observed above 22 T, independent of the field angle.

The main observation is that most anomalies observed in the field dependence of the transport properties (see Figs. 1 and 2) coincide with abrupt changes in the quantum oscillation frequencies and effective masses (see Table 1 in Supplemental Material). They are related to modifications of the FS topology with the most drastic change occurring at H_4 where the Hall effect collapses and $S(H)$ has a pronounced minimum. The FS can be easily modified by applying a magnetic field and the small FS pockets disappear through a LT. We can estimate the characteristic energy of each detected pocket with $\epsilon_i = \hbar^2 k_{F,i}^2/2m_i^\star \approx \hbar e F_i/m_i^\star c$ and we find $\epsilon_\gamma \approx 2.5$ meV, $\epsilon_\omega \approx 5$ meV and $\epsilon_\alpha \approx 6.6$ meV. These energies can be compared to the Zeeman energy scale of a free electron divided by field, $\epsilon_Z/\mu_0 H = g\mu_B \approx 0.12$ meV/T for $g = 2$. As UCoGe is a weak ferromagnet this effect will even be strengthened by the internal field. Hence an important polarization of the bands can be achieved by easily accessible magnetic fields and thus a series of magnetic field-induced LT appears.

The magnetization up to 50 T [26] has a strongly non-linear field dependence suggesting that the electronic magnetic response must vary strongly with the magnetic field while the FM fluctuations are already fully suppressed for $H > 1$ T along the c axis [24, 30]. Thus the electronic instabilities seem to occur in the paramagnetic regime without any additional phase transitions and far above the field where the FM intersite magnetic correlations collapse. The key phenomenon is that FS changes are induced by crossing some critical values of magnetic polarization. In some systems such FS changes are accompanied by a metamagnetic-like transition depending on the nature of the electronic instability. Very recent magnetization measurements [38] point to a tiny metamagnetic-like transition at H_2 but do not detect any anomaly at H_1 and the high field measurements [26] exclude it for H_4 and H_5. The case of UCoGe can be compared to the series of FS reconstructions observed inside the hidden order phase of URu_2Si_2. In this compound no detectable effects on the bulk magnetization have been observed [39], but the LTs are related to the polarization of the small FS pockets [22, 40, 41]. In $CeRu_2Si_2$ the LT is linked to the pseudo-metamagnetic transition where one spin-split FS vanishes continuously at the transition [17, 42], while in $YbRh_2Si_2$ the LT [20, 43] goes along with a suppression of the local Kondo effect as has been demonstrated by renormalized band structure calculations under magnetic field [21]. Recently, a LT occurring at 28 T has been reported in paramagnetic $CeIrIn_5$ [44].

Different LDA band structure calculations have been performed on UCoGe [45, 46] showing strong differences in the FS topology. In the paramagnetic state three bands are contributing to FS sheets with rather small volume, characteristic for a low carrier or semimetallic system. Two cigar-like [45] or pillar-like [46] electron FSs centered around the S point have been predicted which may correspond to the small FSs observed below H_2. In Ref. 45 the FM state with a magnetic polarization along the c axis has also been calculated. The FSs (with a moment of $-0.47\mu_B$/U much larger than in experiment) differ significantly from the paramagnetic ones and do not at all agree with our experiment. In ARPES experiments at zero field details of the FS could not be resolved up to now [46] and it will be of great interest to see the differences of the FS above and below T_C.

In conclusion, we give clear evidences by quantum oscillation experiments for FS instabilities under magnetic field in UCoGe for field along the easy magnetization axis. The occurrence of several LTs under field in the polarized phase of UCoGe shows that FS properties of heavy fermion systems can be easily tuned by magnetic field. The LTs are decoupled from intersite correlations and seem to be driven only by changes in the local fluctuations induced by reaching a critical magnetic polarization. It unveils a strong interplay between magnetic polarization and FS topology, which is directly linked with the dual localized and itinerant nature of the $5f$ electrons. A key challenge in theory is now to take into account the feedback between polarization and FS to model the influence of the magnetic field on the electronic structure.

We thank J.-P. Brison, B. Wu, V. P. Mineev,

A. A. Varlamov and G. Zwicknagl for fruitful discussions. This work has been supported by the ERC grant "NewHeavyFermion", and KAKENHI (25247055,15H05884,15H05882,15K21732, 16H04006), the EuromagNET II (EU contract no. 228043), LNCMI-CNRS is member of the European Magnetic Field Laboratory (EMFL).

* gael.bastien@cea.fr
† georg.knebel@cea.fr

[1] I. M. Lifshitz, Zh. Eksp. Teor. Fiz **38**, 1569 (1960), [Sov, Phys. JETP **1**1, 1130 (1960)].
[2] Y. M. Blanter, M. I. Kaganov, A. V. Pantsulaya, and A. A. Varlamov, Phys. Rep. **245**, 159 (1994).
[3] Y. Yamaji, T. Misawa, and M. Imada, J. Phys. Soc. Jpn. **75**, 094719 (2006).
[4] P. Schlottmann, Phys. Rev. B **83**, 115133 (2011).
[5] M. Bercx and F. F. Assaad, Phys. Rev. B **86**, 075108 (2012).
[6] S. Hoshino and Y. Kuramoto, Phys. Rev. Lett. **111**, 026401 (2013).
[7] A. Benlagra and M. Vojta, Phys. Rev. B **87**, 165143 (2013).
[8] K. Kubo, J. Phys. Soc. Jpn. **84**, 094702 (2015).
[9] M. R. Norman, J. Lin, and A. J. Millis, Phys. Rev. B **81**, 180513 (2010).
[10] D. LeBoeuf, N. Doiron-Leyraud, B. Vignolle, M. Sutherland, B. J. Ramshaw, J. Levallois, R. Daou, F. Laliberté, O. Cyr-Choinière, J. Chang, Y. J. Jo, L. Balicas, R. Liang, D. a. Bonn, W. N. Hardy, C. Proust, and L. Taillefer, Phys. Rev. B **83**, 054506 (2011).
[11] C. Liu, T. Kondo, R. M. Fernandes, A. D. Palczewski, E. D. Mun, N. Ni, A. N. Thaler, A. Bostwick, E. Rotenberg, J. Schmalian, S. L. Bud'ko, P. C. Canfield, and A. Kaminski, Nature Phys. **6**, 419 (2010).
[12] Y. Wang, M. N. Gastiasoro, B. M. Andersen, M. Tomić, H. O. Jeschke, R. Valentí, I. Paul, and P. J. Hirschfeld, Phys. Rev. Lett. **114**, 097003 (2015).
[13] T. Jarlborg and A. Bianconi, Sci. Rep. **6**, 24816 (2016).
[14] E. A. Yelland, J. M. Barraclough, W. Wang, K. V. Kamenev, and A. D. Huxley, Nature Phys. **7**, 890 (2011), arXiv:1107.4471.
[15] C.-C. Liu, J.-J. Zhou, Y. Yao, and F. Zhang, Phys. Rev. Lett. **116**, 066801 (2016).
[16] M. A. Silaev, E. V. Thuneberg, and M. Fogelström, Phys. Rev. Lett. **115**, 235301 (2015).
[17] R. Daou, C. Bergemann, and S. R. Julian, Phys. Rev. Lett. **96**, 026401 (2006).
[18] N. Harrison, S. E. Sebastian, C. H. Mielke, A. Paris, M. J. Gordon, C. A. Swenson, D. G. Rickel, M. D. Pacheco, P. F. Ruminer, J. B. Schillig, J. R. Sims, a. H. Lacerda, M.-T. Suzuki, H. Harima, and T. Ebihara, Phys. Rev. Lett. **99**, 056401 (2007).
[19] S. E. Sebastian, N. Harrison, C. D. Batista, S. a. Trugman, V. Fanelli, M. Jaime, T. P. Murphy, E. C. Palm, H. Harima, and T. Ebihara, Proc Natl Acad Sci U S A **106**, 7741 (2009).
[20] P. M. C. Rourke, A. McCollam, G. Lapertot, G. Knebel, J. Flouquet, and S. R. Julian, Phys. Rev. Lett. **101**, 237205 (2008).
[21] H. Pfau, R. Daou, S. Lausberg, H. R. Naren, M. Brando, S. Friedemann, S. Wirth, T. Westerkamp, U. Stockert, P. Gegenwart, C. Krellner, C. Geibel, G. Zwicknagl, and F. Steglich, Phys. Rev. Lett. **110**, 256403 (2013).
[22] A. Pourret, A. P. Morales, S. Kr"amer, L. Malone, M. Nardone, D. Aoki, G. Knebel, and J. Flouquet, J. Phys. Soc. Jpn. **82**, 034706 (2013).
[23] N. T. Huy, A. Gasparini, D. E. de Nijs, Y. Huang, J. C. P. Klaasse, T. Gortenmulder, A. de Visser, A. Hamann, T. Görlach, and H. v. Löhneysen, Phys. Rev. Lett. **99**, 067006 (2007).
[24] D. Aoki, T. D. Matsuda, F. Hardy, C. Meingast, V. Taufour, E. Hassinger, I. Sheikin, C. Paulsen, G. Knebel, H. Kotegawa, and J. Flouquet, J. Phys. Soc. Jpn. **80**, SA008 (2011).
[25] N. T. Huy, D. E. de Nijs, Y. K. Huang, and A. de Visser, Phys. Rev. Lett. **100**, 077002 (2008).
[26] W. Knafo, T. D. Matsuda, D. Aoki, F. Hardy, G. W. Scheerer, G. Ballon, M. Nardone, A. Zitouni, C. Meingast, and J. Flouquet, Phys. Rev. B **86**, 184416 (2012).
[27] D. Aoki, I. Sheikin, T. D. Matsuda, V. Taufour, G. Knebel, and J. Flouquet, J. Phys. Soc. Jpn. **80**, 013705 (2011).
[28] E. Steven, A. Kiswandhi, D. Krstovska, J. S. Brooks, M. Almeida, A. P. Gonalves, M. S. Henriques, G. M. Luke, and T. J. Williams, Appl. Phys. Lett. **98**, 132507 (2011).
[29] T. V. Bay, A. M. Nikitin, T. Naka, A. McCollam, Y. K. Huang, and A. de Visser, Phys. Rev. B **89**, 214512 (2014).
[30] T. Hattori, Y. Ihara, Y. Nakai, K. Ishida, Y. Tada, S. Fujimoto, N. Kawakami, E. Osaki, K. Deguchi, N. K. Sato, and I. Satoh, Phys. Rev. Lett. **108**, 066403 (2012).
[31] Supplemental Material describes the experimental details, the analysis of the quantum oscillations, and summarizes the quantum oscillation frequencies and effective masses. Supplemental Material includes Refs. [32, 33].
[32] A. Pantsulaya and A. Varlamov, Phys. Lett. A **136**, 317 (1989).
[33] A. Palacio Morales, A. Pourret, G. Knebel, G. Bastien, V. Taufour, D. Aoki, H. Yamagami, and J. Flouquet, Phys. Rev. B **93**, 155120 (2016).
[34] From the opposite sign of ρ_{xy} and S it seems that both quantities are sensitive to differrent charge carriers. However, UCoGe is a compensated metal with equal carrier numbers of holes and electrons. As it is a multiband system it is difficult to conclude on dominant charge carriers. Furthermore, as shown for URhGe in Ref. 47 the sign of S may also depend on the current direction.
[35] B. Wu and et al, (2016), private communication.
[36] D. Aoki and J. Flouquet, J. Phys. Soc. Jpn. **83**, 061011 (2014).
[37] D. Aoki, A. Gourgout, A. Pourret, G. Bastien, G. Knebel, and J. Flouquet, C. R. Phys. **15**, 630 (2014).
[38] A. Nakamura, (2016), private communication.
[39] G. W. Scheerer, W. Knafo, D. Aoki, G. Ballon, A. Mari, D. Vignolles, and J. Flouquet, Phys. Rev. B **85**, 094402 (2012).
[40] M. M. Altarawneh, N. Harrison, S. E. Sebastian, L. Balicas, P. H. Tobash, J. D. Thompson, F. Ronning, and E. D. Bauer, Phys. Rev. Lett. **106**, 146403 (2011).
[41] L. Malone, L. Howald, A. Pourret, D. Aoki, V. Taufour, G. Knebel, and J. Flouquet, Phys. Rev. B **85**, 024526

(2012).
[42] M. Boukahil, A. Pourret, G. Knebel, D. Aoki, Y. Ōnuki, and J. Flouquet, Phys. Rev. B **90**, 075127 (2014).
[43] A. Pourret, G. Knebel, T. D. Matsuda, G. Lapertot, and J. Flouquet, J. Phys. Soc. Jpn. **82**, 053704 (2013).
[44] D. Aoki, G. Seyfarth, A. Pourret, A. Gourgout, A. McCollam, J. A. N. Bruin, Y. Krupko, and I. Sheikin, Phys. Rev. Lett. **116**, 037202 (2016).
[45] M. Samsel-Czekała, S. Elgazzar, P. M. Oppeneer, E. Talik, W. Walerczyk, and R. Troć, J. Phys.: Condens. Matter **22**, 015503 (2010).
[46] S.-i. Fujimori, T. Ohkochi, I. Kawasaki, A. Yasui, Y. Takeda, T. Okane, Y. Saitoh, A. Fujimori, H. Yamagami, Y. Haga, E. Yamamoto, and Y. Ōnuki, Phys. Rev. B **91**, 174503 (2015).
[47] A. Gourgout, A. Pourret, G. Knebel, D. Aoki, G. Seyfarth, and J. Flouquet, Phys. Rev. Lett. **117**, 046401 (2016).

SUPPLEMENTAL MATERIAL

Single crystal growth

High quality single crystals of UCoGe (orthorhombic TiNiSi structure) were grown in a tetra-arc furnace by the Chzochralski method and further annealed. Two single crystals have been cut by spark erosion. The orientation of the single crystals have been checked by Laue diffraction. Sample S1 has a residual resistivity ratio $[RRR = \rho(300\,\mathrm{K})/\rho(1\,\mathrm{K})]$ of 105 and sample S2 of 36.

Experimental details

Resistivity measurements were performed under high magnetic field in a 34 T resistive magnet at the high magnetic field facilility LNCMI Grenoble. The samples were mounted on a one axis mechanical rotator and cooled in a top loading dilution refrigerator down to 40 mK. The resistivity was measured with the usual four probe ac current method. The electrical current was below 200 μA. More accurate measurements were performed in CEA in a 13 T superconducting magnet. Sensitivity was enhanced compared to the high field set up by the use of a low temperature transformer thermalized at the 1 K stage of the dilution refrigerator. These measurements were performed down to 30 mK and electrical current was reduced down to 50 μA.

Thermoelectric power measurements under high magnetic field were performed in LNCMI Grenoble, with a ^{3}He cryostat down to 400 mK and with a resistive magnet up to 34 T. Lower temperature measurements were done in a superconducting magnet up to 16 T and with a home-made dilution fridge down to 0.1 K. To determine the angular dependence of H_1 in the bc-plane an Attocube piezorotator has been used to rotate the sample in the magnetic field.

The thermopower has been measured with an "one heater two thermometers" set up. The RuO_2 thermometers had been calibrated against a Ge thermometer which is installed in the field-compensated zone of the superconducting magnet. Both thermometers and the heater are thermally decoupled from the heat bath of the sample holder by highly resistive manganine wires with specific resistance of 200 Ω/m. To measure quantum oscillations the field has been swept continuously upwards. A constant power has been used to heat the sample. The thermoelectric voltage had been taken at the beginning and the end of the field sweeps to estimate the background signal.

Quantum oscillations

To extract the oscillating part of the magnetoresistance (see Fig. 2 of the article), a Loess algorithm has been used to average the oscillations and the smoothed curve has been subtracted from the data. As in the thermoelectric signal the different anomalies are very marked and the signal is very non-monotonous, we subtracted the data at $T = 1.2$ K where no oscillations but still the anomalies are visible. Then, we determined the envelope of the remaining signal and subtracted the average of the upper and lower envelope. This was cross-checked by subtracting a polynomial background on a reduced window. The quantum oscillation frequencies have been determined by fast Fourier transformation (FFT) in the respective field windows between the different anomalies. The change of the FFT frequencies has been also confirmed by performing a FFT on sliding windows in $1/H$.

Table I gives the quantum oscillation frequencies and the effective masses for field along the c axis in the respective field intervals between the different anomalies. While the temperature dependence of the amplitude of the SdH oscillations follow the Lifshitz Kosevich formula, the amplitude of the thermoelectric power oscillations is given by the derivative of the Lifshitz Kosevich formula [32, 33]. A very good agreement was observed between quantum oscillation frequencies observed on the different samples with resistivity and with thermopower on S1 and a relatively good agreement for the effective masses.

TABLE I. Quantum oscillations frequencies and effective masses in UCoGe from resistivity and Seebeck effect measurements for field along the c axis. Different field intervals are considered, they are delimited by the anomalies observed in transport measurements.

		SdH(sample1)		SdH(sample2)		Seebeck(sample1)	
H range	orbit	F(T)	$m^*(m_0)$	F(T)	$m^*(m_0)$	F(T)	$m^*(m_0)$
4T $< H <$ 9T	γ			230	7		
	β	270		280		285	
9T $< H <$ 16T	γ	240	11	240	8	240	12
	β	310	11	310	11	310	13
16T $< H <$ 21T	ω					600	14
23T $< H$	α	970	17	955		980	14